A Ni(I)Fe(II) analogue of the Ni-L state of the Active Site of the [NiFe] Hydrogenases

Carlo U. Perotto[a], George Marshall[a], Graham J. Jones[a], E. Stephen Davies[a], William Lewis[a], Jonathan McMaster[a,*] and Martin Schröder[a,b,*].

[

$Ni(L^1)Fe(^tBuNC)_4](PF_6)_2$ is a robust $Ni^{II}Fe^{II}$ complex that undergoes a reversible one-electron reduction. Spectroscopic and theoretical studies show that $[Ni(L^1)Fe(^tBuNC)_4]^+$ is an unprecedented $Ni^{I}Fe^{II}$ species that reproduces the electronic configuration of the Ni-L state of the [NiFe] hydrogenases.

a. The University of Nottingham, University Park, Nottingham, NG7 2RD, UK. Email: j.mcmaster@nottingham.ac.uk

b. The University of Manchester, Oxford Road, Manchester, M13 9PL, UK. Email: m.schroder@manchester.ac.uk

The [NiFe]-hydrogenases catalyse the two-electron inter-conversion of two protons and molecular hydrogen.[1] The nature of the Ni-Fe heterobimetallic active site in these enzymes is now established; the Ni centre is co-ordinated by two terminal and two bridging cysteinate donors, which co-ordinate to a Fe centre that is also bound by one carbonyl and two cyanide ligands (Scheme 1). Catalytic H_2 cleavage is associated with changes in the formal oxidation state of the Ni centre while the Fe centre remains in the Fe^{II} state during turnover.[1c] Three key states have been identified in a catalytic cycle (Scheme 1): Ni-SI, Ni-R and Ni-C. Thus, H_2 reacts with Ni-SI and undergoes heterolytic cleavage to form Ni-R which contains a bridging H^- ligand. A co-ordinated Cys ligand may act as an initial proton acceptor for the accompanying proton before its transfer to other bases (B) about the active site.[3] The removal of an electron generates the EPR active S = ½ Ni-C state, which can be converted to an EPR-active S = ½ Ni^IFe^{II} state (Ni-L) following the photolysis at low temperatures.[4] Previously, Ni-L had not been viewed as being catalytically relevant given the conditions required for its formation. However, recent *in situ* IR spectroelectrochemical studies have demonstrated that Ni-L may be generated reversibly in the dark under turnover conditions.[2] Therefore, the regeneration of the Ni-SI state could occur either directly from the Ni-C state, via the concerted transfer of an electron and a proton, or by oxidation of the Ni-L state. These studies, together with previous DFT calculations,[5] open up the possibility that separate proton and electron transfer events may be associated with the regeneration of the Ni-SI state from Ni-C, and that these steps may involve the Ni-L state (Scheme 1). Despite the large number of diamagnetic $Ni^{II}Fe^{II}$ complexes that have been prepared as analogues of the [NiFe] hydrogenases,[6] the syntheses of paramagnetic analogues have proven to be more challenging.[7] Several $Ni^{III}Fe^{III}$, $Ni^{II}Fe^{III}$, $Ni^{II}Fe^{I}$ and $Ni^{I}Fe^{I}$ centres have been reported,[6c,7-8] none of which have succeeded in reproducing the crucial Ni^IFe^{II} and $Ni^{III}Fe^{II}$ states found for the [NiFe] hydrogenases. For example, [(dppe)Ni(μ-pdt)$Fe(CO)_3$](BF_4)[7] [dppe = 1,2-bis(diphenylphos-phino)ethane, pdt = propane-1,2-dithiolate] possesses a $Ni^{II}Fe^{I}$ configuration with spin density localized principally on the Fe centre and

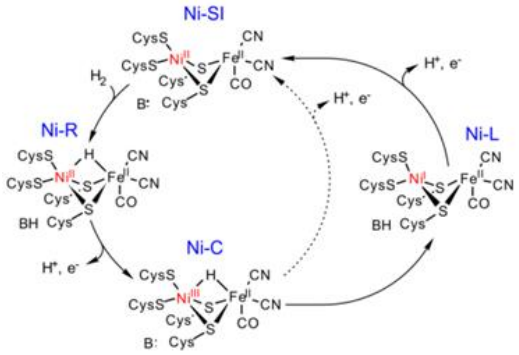

Scheme 1: A proposed catalytic cycle for H_2 oxidation by the [NiFe] hydrogenases showing regeneration of Ni-SI directly from Ni-C (dotted line) or via a recently proposed route involving Ni-L (solid line).[2]

[(dppe)Ni(μ-pdt)Ru(cymene)][9] possesses a $Ni^{I}Ru^{II}$ centre rather than the biologically more relevant $Ni^{I}Fe^{II}$ unit. Given the renewed focus on the role of Ni-L, we report the characterisation of a $Ni^{I}Fe^{II}$ complex ($[\mathbf{1}]^{+}$) as an analogue of this state. $[\mathbf{1}]^{+}$ is prepared from the reversible, one-electron reduction of the parent complex $[\mathbf{1}]^{2+}$ (Fig. 1). Our assignment of $[\mathbf{1}]^{+}$ as a $Ni^{I}Fe^{II}$ centre represents the first analogue of the Ni-L form of the [NiFe] hydrogenases to feature Ni and Fe centres with electronic configurations that mirror those proposed for Ni-L.

Treatment of a solution of $[Ni(L^{1})]$ (H_2L^{1} = N,N'-diethyl-3,7-diazanonane-1,9-dithiol)[10] in acetonitrile with $FeCl_2$ followed by the addition of four equivalents of ^{t}BuNC and NH_4PF_6 affords $[Ni(L^{1}N_2S_2)Fe(^{t}BuNC)_4](PF_6)_2$ ($[\mathbf{1}](PF_6)_2$). $[\mathbf{1}](PF_6)_2$ is stable at room temperature in air as a solid and in acetonitrile solution for at least 48 h, as monitored by IR spectroscopy. The crystallographic characterization of $[\mathbf{1}](PF_6)_2\cdot$MeCN shows the Ni centre in an approximate square-planar N_2S_2 environment with Fe having a pseudo-octahedral co-ordination sphere comprised of four ^{t}BuNC ligands and two S donors derived from $[Ni(L^{1})]$ (Fig. 1). The NiN_2S_2 fragment retains the structural features of the $[Ni(L^{1})]$ precursor,[11] the most significant difference being a smaller S(1)-Ni(1)-S(2) angle [81.76(2)°] in $[Ni(L^{1})]$ relative to that in $[\mathbf{1}]^{2+}$ [84.20(2)°]. This difference may reflect the steric demands of the co-ordinated $[Fe(^{t}BuNC)_4]^{2+}$

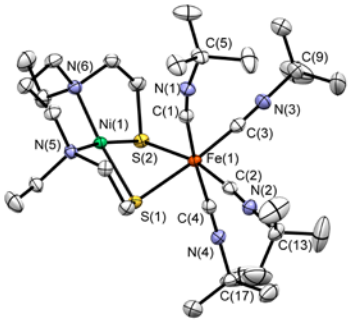

Fig. 1: X-Ray structure of the cation $[\mathbf{1}]^{2+}$ in $[1](PF_6)_2$ with 50% probability thermal ellipsoids.

fragment in $[\mathbf{1}]^{2+}$. The equatorial ^{t}BuNC ligands defined by C(2) and C(3) bind to Fe(1) in an essentially linear mode with Fe(1)-C-N angles of 175.3(2)° and 175.1(2)°, respectively. In contrast the axial ^{t}BuNC ligands, defined by C(1) and C(4), co-ordinate in a bent geometry with Fe(1)-C-N angles of 170.0(2) and 172.9(2)°, respectively. The Ni(1)-C(1) and Ni(1)-C(4) distances [2.951(2) and 4.164(2) Å, respectively] are significantly greater than the Fe(1)-C(1) and Fe(1)-C(4) distances [1.890(2) and 1.888(2) Å, respectively]. Thus, the axial ^{t}BuNC ligands do not appear to adopt bridging modes between the Ni and Fe centres in $[\mathbf{1}]^{2+}$ and the non-linear binding mode of these ligands about Fe(1) may result from inter- and intra-molecular interactions due to crystal packing (Fig. S1). The Ni(1)-Fe(1) distance [2.9898(7) Å] compares well with that in the inactive oxidised form of [NiFe] hydrogenase from *Desulfovibrio gigas* (2.9 Å)[12] and is significantly longer than that found in the Ni-R form from *Desulfovibrio vulgaris* Miyazaki F (2.57 Å)[3a] that both contain Ni and Fe in formal M^{II} oxidation states.

The cyclic voltammogram of $[\mathbf{1}](PF_6)_2$, recorded at 298K in MeCN containing 0.2 M $[N^nBu_4][BF_4]$ as supporting electrolyte, shows a reduction process at $E_{1/2}$ = -1.39 V *vs* Fc^+/Fc that is reversible over the range of scan rates employed in the experiment (20 – 300 mVs^{-1}, Figs. S2 and S3). The cyclic voltammogram of $[Ni(L^1)]$ recorded under the same conditions reveals a reduction process at E_p^c = -2.35 V *vs* Fc^+/Fc (Fig S4), assigned to the reduction of $[Ni(L^1)]$ to the formal Ni^I state on the

basis of comparisons with previously reported NiN_2S_2 complexes possessing similar co-ordination spheres.[13] The shift of *ca.* +1 V for the reduction of [**1**]$(PF_6)_2$ relative to that of [Ni(L^1)] is consistent with the formation of a Lewis base Lewis acid adduct between [Ni(L^1)] and [Fe(^{t}BuNC)$_4$]$^{2+}$; *ca.* +0.5 V shifts in potential have been observed previously for (NiN_2S_2)W(CO)$_4$ relative to their parent NiN_2S_2 complexes.[13] UV/Vis spectroelectrochemistry indicates that [**1**]$^+$ decomposes at temperatures above 273 K and that cooling to 243K is required to ensure the quantitative regeneration of [**1**]$^{2+}$ (Fig. S5, Table S1). On cooling to 243 K the cyclic voltammogram of [**1**]$(PF_6)_2$ becomes electrochemically irreversible (Fig. S6) and the controlled potential electrolysis of [**1**]$(PF_6)_2$ at -1.6 V *vs* Fc^+/Fc at 243K confirms that a one-electron reduction process accompanies the formation of [**1**]$^+$. The cyclic voltammograms of [**1**]$(PF_6)_2$ and [**1**]$^+$ at 243K exhibit similar profiles confirming the stability of [**1**]$^+$ under the conditions and timescale of the experiment (Fig. S7).

The IR spectra of [**1**]$(PF_6)_2$ and [**1**]$^+$ in MeCN solution are shown in Fig. 2. Each spectrum exhibits four bands assigned to the C-N stretches of the ^{t}BuNC ligands. In [**1**]$^{2+}$ these bands occur at frequencies typical of isonitrile ligands bound in a terminal mode to transition metal centres.[14] The overall shift of the bands to lower frequencies following the reduction of [**1**]$^{2+}$ to [**1**]$^+$ is consistent with an increase in the electron density about the Ni-Fe core and a corresponding increase in π-back-donation into the ^{t}BuNC units. A C-N stretching band at 1857 cm^{-1} in the IR spectrum of [**1**]$^+$ in MeCN solution suggests that one terminal, apical ^{t}BuNC ligand moves to a bridging mode between the Ni and Fe centres (Fig. 2) following the reduction of [**1**]$^{2+}$; a similar bridging mode is found in $[Fe_2(pdt)(MeNC)_7](PF_6)_2$ where one MeNC ligand bridges between the two Fe centres.[15]

The X-band EPR spectrum of electrochemically generated [**1**]$^+$ recorded at 77 K in MeCN / 0.2 M $[N^nBu_4][BF_4]$ (Fig. 3a) shows striking similarities to those of Ni$^I N_2S_2$ complexes (*S* = thiolato, thioether or sulfonato, *N* = amine donors; $g_\parallel$ = 2.18 – 2.25; $g_\perp$ = 2.057-2.071), generated by

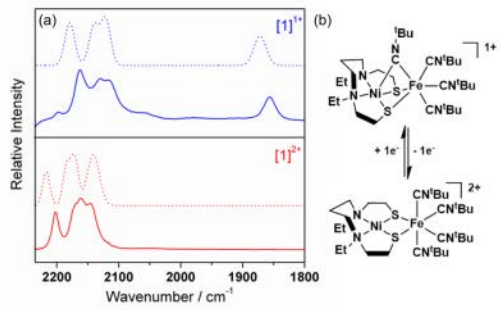

Fig. 2: (a) solution IR spectra of [**1**](PF$_6$)$_2$ (2200, 2170, 2161 and 2144 cm^{-1}) and [**1**]$^+$ (2162, 2129, 2116 and 1857 cm^{-1}) recorded in MeCN (solid lines) and DFT calculated spectra (dotted lines; 2216, 2183, 2169, 2139 cm^{-1} for [**1**]$^{2+}$ and 2179, 2140, 2121, 1872 for [**1**]$^+$). (b) proposed rearrangement supported by DFT calculations.

chemical reduction of their Ni^{II} counterparts,[16] and, crucially, is substantially different to those of Fe^I centres including [Fe(CO)$_3$(PPh$_3$)$_2$]$^+$ (g_{xx} = 2.053, g_{yy} = 2.090, g_{zz} = 2.001)[17] and [(dppe)Ni(μ-pdt)Fe(CO)$_3$]$^+$ (g_{xx} = 2.052, g_{yy} = 2.050, g_{zz} = 2.005 for one isomer).[7] Thus, the EPR spectroscopic data are consistent with a formal Ni^{I}Fe^{II} unit in [**1**]$^+$ where the Ni^I centre adopts a d^9, S = ½ configuration in which the unpaired electron resides in d-orbital orientated in the equatorial plane of the Ni^I*N*$_2$*S*$_2$ unit with associated spin Hamiltonian parameters $g_{zz} > g_{xx} \approx g_{yy} > g_e$.[18] In contrast, the Ni-L form of the [NiFe] hydrogenases is characterised by a rhombic EPR spectrum (g_{11} = 2.30, g_{22} = 2.12 and g_{33} = 2.05)[19] that may be viewed as resulting from the re-hybridization of the Ni $d_{x^2-y^2}$ and d_{z^2} orbitals in Ni-C where one hybrid contributes to a Ni-Fe bond.[20] The UV/vis spectrum of [**1**]$^+$ (Table S1 and Fig. S5) shows bands at 400 (3900), 490 (1760), 520 (1500), 598 (1100) and 720 nm (380 M^{-1} cm^{-1}) that are consistent with those in the UV/vis spectra of other well-defined Ni^I complexes.[21]

In order to support the Ni^{I}Fe^{II} assignment proposed for [**1**]$^+$, we conducted density functional theory (DFT) calculations on the full structures of [**1**]$^{2+/+}$. The calculated structure of [**1**]$^{2+}$ [Fig. S8(a)] reproduces the principal features of the experimentally determined structure (Fig. 1); the average Fe-C distances are *ca.* 0.02 Å shorter and the Ni-S and Fe-S distances are *ca.* 0.04 Å longer in the calculated structure of [**1**]$^{2+}$ (Table S3). The principal differences between the calculated and

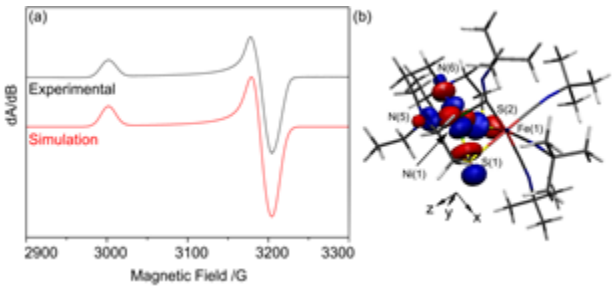

Fig. 3: (a) X-band EPR spectrum of $[\mathbf{1}]^{+}$ as a solution in MeCN/0.2 M $[N^{n}Bu_4][BF_4]$ at 77 K. Experimental (black) and simulated (red) spectrum, simulated using the spin Hamiltonian parameters g_{11} = 2.210, $g_{22} = g_{33}$ = 2.074 (W_{11} = 18, W_{22} = 16, W_{33} = 17 G); (b) The Kohn-Sham SOMO of $[\mathbf{1}]^{+}$ plotted with an isosurface value of 0.05 eÅ^{-3}.

experimental structures are (i) a relaxation of the dihedral angle defined by the S(1)-Ni(1)-S(2) and S(1)-Fe(1)-S(2) planes [117.94(3)° and 128.3°, in the calculated and experimental structures, respectively], (ii) an increase in the Ni(1)-Fe(1) distance of *ca* 0.2 Å in the calculated relative to the experimental structure of $[\mathbf{1}]^{2+}$ [Ni(1)-Fe(1) = 3.209 Å and 2.9896(4) Å for the calculated and experimental structures, respectively, Table S2], and (iii) an increase in the of the C-Fe(1)-C and Fe(1)-C-N angles for the axial ^{t}BuNC ligands defined by C(1) and C(4) (Table S2). The unscaled[22] calculated IR spectrum of $[\mathbf{1}]^{2+}$ possesses four bands in the C-N stretching region at 2216, 2183, 2169 and 2139 cm^{-1} that compare well with the experimental stretching frequencies (Fig. 2). Thus, the close correspondence between the calculated and experimental structures, and IR spectra suggest that the DFT calculations provide a reasonable description of the geometric and electronic structure of $[\mathbf{1}]^{2+}$. The composition[23] of the HOMO in $[\mathbf{1}]^{2+}$ shows that it is largely metal-centred [59.3% Ni d_{z^2}, 0.6% Ni d_{xz}, 9.7% Fe $d_{x^2-y^2}$, 1.2% Fe d_{xz}, S 25.8%, N(5)+N(6) 1.2%, Fig. S9] The Mayer bond order[24] between the Ni(1) and Fe(1) centres (0.04) derived from the DFT calculations suggests there is no formal metal-metal bond in $[\mathbf{1}]^{2+}$. Overall the description of the electronic structure of $[\mathbf{1}]^{2+}$ is consistent with an S = 0 $Ni^{II}Fe^{II}$ centre in $[\mathbf{1}]^{2+}$.

The calculated structure of $[\mathbf{1}]^{+}$ suggests that significant changes in geometry about the Ni(1) and Fe(1) centres accompany the reduction of $[\mathbf{1}]^{2+}$ [Fig. S8(b) and Table S3] These include a marked decrease in the dihedral angle between the S(1)-Ni(1)-S(2) and S(1)-Fe(1)-S(2) planes (94.1° and 128.3°, for $[\mathbf{1}]^{+}$ and $[\mathbf{1}]^{2+}$, respectively) and a shortening of the Ni(1)-Fe(1) distance [Ni(1)-Fe(1) = 2.616 Å and 3.209 Å for $[\mathbf{1}]^{1+}$ and $[\mathbf{1}]^{2+}$, respectively], which compares well with that calculated for models of the active site of the Ni-L form.[20] On the reduction of $[\mathbf{1}]^{2+}$ one axial ^{t}BuNC ligand, defined by C(1), moves to a bridging mode between the Fe(1) and Ni(1) centres with Fe(1)-C(1) and Ni(1)-C(1) distances of 1.942 and 2.018 Å, respectively. The adoption of a bridging mode for this ligand is accompanied by a significant bend in the backbone of the ligand [C(1)-N(1)-C(5) = 140.9°], which is commonly observed for bridging isocyanides.[25] The calculated IR spectrum for $[\mathbf{1}]^{+}$ shows three intense C-N stretches at 2179, 2140 and 2121 cm^{-1} for the terminal isocyanides and a single band at 1872 cm^{-1} for the C-N stretching mode of the bridging ^{t}BuNC ligand. This calculated spectrum shows close correspondence to the experimental IR spectrum of $[\mathbf{1}]^{+}$ (Fig. 2) and strongly supports a structural rearrangement in which a terminal ^{t}BuNC ligand moves to a bridging mode on the reduction of $[\mathbf{1}]^{2+}$. This structural rearrangement may also underpin the differences in profiles of the cyclic voltammograms of $[\mathbf{1}](PF_6)_2$ recorded at 298 K (Fig. S2) and 243K (Fig. S6). The rate of the suggested structural rearrangements for $[\mathbf{1}]^{2+/+}$ may be slowed at 243K with the consequent loss of electrochemical reversibility for the $[\mathbf{1}]^{2+/+}$ process at 243K. We are unable to determine the precise mechanism that gives rise to the voltammetric profile *i.e.* whether electron transfer precedes structural rearrangement or *vice versa*. However, the results of the UV/vis spectroelectrochemical experiments clearly show that the process is chemically reversible at 243K over the timescale of this experiment.

The SOMO of $[\mathbf{1}]^{+}$ possesses 60.8% Ni d_{xy}, 1.3% Ni d_{xz}, 1.1% Ni d_{yz} S 21.7%, N(5)+N(6) 10.2% character and is essentially localized on the NiN_2S_2 unit (Fig. 3b). The calculated EPR spin

Hamiltonian parameters using the BP86 functional (g_{zz} = 2.174, g_{yy} = 2.079, g_{xx} = 2.070, Table S2) reproduce the approximately axial nature of the frozen solution EPR spectrum of [**1**]$^{+}$ (Fig. 3a). We note that the DFT calculations underestimate the largest g-shift (g_{zz} = 2.174 calc. *vs* g_{11} = 2.210). Such underestimations (by up to 30%) have been observed previously for various metal centres including Ni^{I}, and these underestimations have been attributed partly to overestimations in spin delocalization into ligand-based orbitals in the calculated electronic structures.[20,26] Thus, these results, together with the excellent agreement between the calculated and experimental IR spectra, support a $Ni^{I}Fe^{II}$ description for [**1**]$^{+}$ where the unpaired electron is essentially localised in the d_{xy} orbital of a d^{9} Ni^{I} centre. The calculated Ni-Fe Mayer bond order increases from 0.04 in [**1**]$^{2+}$ to 0.20 in [**1**]$^{+}$ indicating the development of a Ni-Fe interaction but not a direct bond. In contrast, DFT calculations on models of the Ni-L state possess Ni-Fe bond orders of *ca.* 0.40 supporting the formation of a metal-metal bond in these centres.[20] The absence of a formal Ni-Fe bond in [**1**]$^{+}$ is not surprising given the additional fourth ^{t}BuNC ligand in the co-ordination sphere of Fe^{II} which occupies a bridging position between the Ni and Fe centres; this site is vacant in structures proposed for Ni-L.

Ni-L reacts with CO and converts to the paramagnetic Ni-CO state which features a CO ligand bound to the Ni^{I} centre.[27] Thus, we examined the reactivity of [**1**]$^{2+}$ and [**1**]$^{+}$ towards CO. Whereas [**1**]$^{2+}$ does not react with CO, a solution of [**1**]$^{1+}$ chemically generated from [**1**](PF_6) with [Cp*$_2$Co] readily reacts with CO at 243 K, as monitored by IR spectroscopy (Fig. S10). Several new bands develop in the C-O and C-N stretching region and the frozen solution EPR spectrum exhibits multiple low field features (Fig. S10) suggesting the formation of multiple products, which proved intractable.

In conclusion, [**1**]$^{2+}$ has been prepared and structurally characterized as its [**1**](PF_6)$_2$ salt. The electrochemical one-electron reduction of [**1**]$^{2+}$ generates paramagnetic [**1**]$^{+}$ which has been

characterized by IR, UV/vis and EPR spectroscopies. DFT calculations reproduce the principal features of the IR spectrum of $[\mathbf{1}]^+$ and, in contrast to Ni-L, $[\mathbf{1}]^+$ does not contain a formal Ni-Fe bond. Rather the formation of $[\mathbf{1}]^+$ may be associated with a structural rearrangement that incorporates a bridging ^{t}BuNC ligand between the Ni and Fe centres. The frozen solution X-band EPR spectrum of $[\mathbf{1}]^+$ and DFT calculated spin Hamiltonian parameters are consistent with a SOMO that is largely localized at the NiN_2S_2 core in a Ni d_{xy} orbital. Thus, the experimental and theoretical data supports the assignment of $[\mathbf{1}]^+$ to a mixed-valence Ni^IFe^{II} state. In this respect $[\mathbf{1}]^+$ represents the first example of an Ni-Fe analogue of the active site of the [NiFe] hydrogenases that reproduces the formal oxidation and spin states of the metal centres in the Ni-L form.

We thank EPSRC and the University of Nottingham for support. MS gratefully acknowledges receipt of an ERC advanced grant.

References

1. (a) J. C. Fontecilla-Camps, A. Volbeda, C. Cavazza and Y. Nicolet, *Chem. Rev.*, 2007, **107**, 4273-4303; (b) W. Lubitz, H. Ogata, O. Rüdiger and E. Reijerse, *Chem. Rev.*, 2014, **114**, 4081-4148; (c) H. Ogata, W. Lubitz and Y. Higuchi, *Dalton Trans.*, 2009, **9226**, 7577-7587; (d) A. Volbeda and J. C. Fontecilla-Camps, *Dalton Trans.*, 2003, 4030-4038.

2. R. Hidalgo, P. A. Ash, A. J. Healy and K. A. Vincent, *Angew. Chem. Int. Ed.*, 2015, **54**, 7110-7113.

3. (a) H. Ogata, K. Nishikawa and W. Lubitz, *Nature*, 2015, **520**, 571-574; (b) A. Abou-Hamdan, P. Ceccaldi, H. Lebrette, O. Gutierrez-Sanz, P. Richaud, L. Cournac, B. Guigliarelli, A. L. De Lacey, C. Leger, A. Volbeda, B. Burlat and S. Dementin, *J. Biol. Chem.*, 2015, **290**, 8550-8558.

4. (a) M. Brecht, M. van Gastel, T. Buhrke, B. Friedrich and W. Lubitz, *J. Am. Chem. Soc.*, 2003, **125**, 13075-13083; (b) J. P. Whitehead, R. J. Gurbiel, C. Bagyinka, B. M. Hoffman and M. J. Maroney, *J. Am. Chem. Soc.*, 1993, **115**, 5629-5635.

5. (a) S. Q. Niu, L. M. Thomson and M. B. Hall, *J. Am. Chem. Soc.*, 1999, **121**, 4000-4007; (b) A. Pardo, A. L. De Lacey, V. M. Fernandez, H. J. Fan, Y. B. Fan and M. B. Hall, *J. Biol. Inorg. Chem.*, 2006, **11**, 286-306.

6. (a) S. Canaguier, V. Artero and M. Fontecave, *Dalton Trans.*, 2008, 315-325; (b) J. Dawson, C. Perotto, J. McMaster and M. Schröder, in *Bioinspired Catalysis*, eds. W. Weigand and P. Schollhammer, Wiley-VCH Verlag GmbH & Co., 2014, pp. 79-104; (c) C. Tard and C. J. Pickett, *Chem. Rev.*, 2009, **109**, 2245-2274; (d) P. A. Summers, J. Dawson, F. Ghiotto, M. W. D. Hanson-Heine, K. Q. Vuong, E. S. Davies, X.-Z. Sun, N. A. Besley, J. McMaster, M. W. George and M. Schröder, *Inorg. Chem.*, 2014, **53**, 4430-4439; (e) M. L. Helm, M. P. Stewart, R. M. Bullock, M. R. DuBois and D. L. DuBois, *Science*, 2011, **333**, 863-866; (f) C. H. Lai, J. H. Reibenspies and M. Y. Darensbourg, *Angew. Chem. Int. Ed.*, 1996, **35**, 2390-2393; (g) S. Ogo, K. Ichikawa, T. Kishima, T. Matsumoto, H. Nakai, K. Kusaka and T. Ohhara, *Science*, 2013, **339**, 682-684; (h) K. Weber, T. Kraemer, H. S. Shafaat, T. Weyhermueller, E. Bill, M. van Gastel, F. Neese and W. Lubitz, *J. Am. Chem. Soc.*, 2012, **134**, 20745-20755; (i) C. Wombwell and E. Reisner, *Chem. Eur. J.*, 2015, **21**, 8096-8104.

7. D. Schilter, M. J. Nilges, M. Chakrabarti, P. A. Lindahl, T. B. Rauchfuss and M. Stein, *Inorg. Chem.*, 2012, **51**, 2338-2348.

8. (a) D. Schilter, T. B. Rauchfuss and M. Stein, *Inorg. Chem.*, 2012, **51**, 8931-8941; (b) G. Steinfeld and B. Kersting, *Chem. Commun.*, 2000, 205-206; (c) W. F. Zhu, A. C. Marr, Q. Wang, F. Neese, D. J. E. Spencer, A. J. Blake, P. A. Cooke, C. Wilson, M. Schröder and M. Schröder, *Proc. Natl. Acad. Sci. USA*, 2005, **102**, 18280-18285.

9. G. M. Chambers, J. Mitra, T. B. Rauchfuss and M. Stein, *Inorg. Chem.*, 2014, **53**, 4243-4249.

10.(a) F. Osterloh, W. Saak and S. Pohl, *J. Am. Chem. Soc.*, 1997, **119**, 5648-5656; (b) J. A. Denny and D. M. Y., *Chem. Rev.*, 2015, **115**, 5248-5273.

11.J. Schneider, R. Hauptmann, F. Osterloh and G. Henkel, *Acta Crystallogr. Sect. C-Cryst. Struct. Commun.*, 1999, **55**, 328-330.

12.A. Volbeda, E. Garcin, C. Piras, A. L. De Lacey, V. M. Fernandez, E. C. Hatchikian, M. Frey and J. C. Fontecilla-Camps, *J. Am. Chem. Soc.*, 1996, **118**, 12989-12996.

13.M. V. Rampersad, S. P. Jeffery, M. L. Golden, J. Lee, J. H. Reibenspies, D. J. Darensbourg and M. Y. Darensbourg, *J. Am. Chem. Soc.*, 2005, **127**, 17323-17334.

14.R. Taylor and W. Horrocks, *Inorg. Chem.*, 1964, **3**, 584-589.

15.J. D. Lawrence, T. B. Rauchfuss and S. R. Wilson, *Inorg. Chem.*, 2002, **41**, 6193-6195.

16.P. J. Farmer, J. H. Reibenspies, P. A. Lindahl and M. Y. Darensbourg, *J. Am. Chem. Soc.*, 1993, **115**, 4665-4674.

17.J. H. Macneil, A. C. Chiverton, S. Fortier, M. C. Baird, R. C. Hynes, A. J. Williams, K. F. Preston and T. Ziegler, *J. Am. Chem. Soc.*, 1991, **113**, 9834-9842.

18.(a) A. Lappin and A. McAuley, *Adv. Inorg. Chem.*, 1988, **32**, 241-295; (b) G. Musie, P. J. Farmer, T. Tuntulani, J. H. Reibenspies and M. Y. Darensbourg, *Inorg. Chem.*, 1996, **35**, 2176-2183.

19.S. Foerster, M. Stein, M. Brecht, H. Ogata, Y. Higuchi and W. Lubitz, *J. Am. Chem. Soc.*, 2003, **125**, 83-93.

20.M. Kampa, M.-E. Pandelia, W. Lubitz, M. van Gastel and F. Neese, *J. Am. Chem. Soc.*, 2013, **135**, 3915-3925.

21.(a) L. Gomes, E. Pereira and B. de Castro, *J. Chem. Soc., Dalton Trans.*, 2000, 1373–1379; (b) E. Pereira, L. Gomes and B. de Castro, *J. Chem. Soc., Dalton Trans.*, 1998, 629-636; (c) D. J. Szalda, E. Fujita, R. Sanzenbacher, H. Paulus and H. Elias, *Inorg. Chem.*, 1994, **33**, 5855-5863.

22.J. P. Merrick, D. Moran and L. Radom, *J. Phys. Chem. A*, 2007, **111**, 11683-11700.

23.A. Reed, R. Weinstock and F. Weinhold, *J. Chem. Phys.*, 1985, **83**, 735-746.

24.I. Mayer, *Chem. Phys. Lett.*, 1987, **97**, 270-274.

25.R. D. Adams and F. A. Cotton, *Inorg. Chem.*, 1974, **13**, 249-253.

26.F. Neese, *J. Chem. Phys.*, 2003, **118**, 3939-3948.

27.M.-E. Pandelia, H. Ogata, L. J. Currell, M. Flores and W. Lubitz, *BBA - Bioenergetics*, 2010, **1797**, 304-313.